

Cell Reports

Supplemental Information

**Microtubule-Dependent Mitochondria Alignment  
Regulates Calcium Release in Response  
to Nanomechanical Stimulus in Heart Myocytes**

Michele Miragoli, Jose L. Sanchez-Alonso, Anamika Bhargava, Peter T. Wright, Markus Sikkell, Sophie Schobesberger, Ivan Diakonov, Pavel Novak, Alessandra Castaldi, Paola Cattaneo, Alexander R. Lyon, Max J. Lab, and Julia Gorelik

## Supplemental Information

### Supplemental figures.

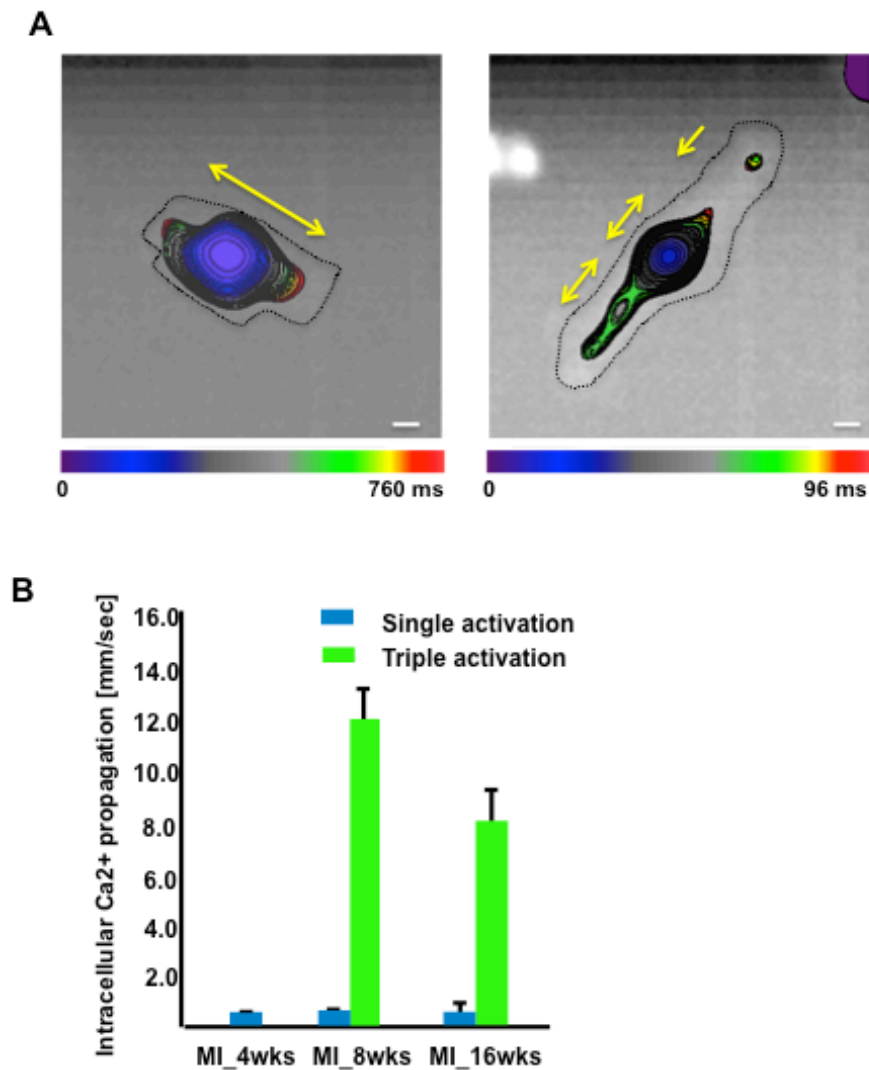


**Figure S1**

**Figure S1**, related to Figure 3

**Propagation of  $MiCa_i$  often evokes initiation of secondary calcium waves at the cell edges. A.** color-coded time-lapse map of  $MiCa_i$  with either single (left) or triple (right) initiation. Bar= 10  $\mu$  **B.** Intracellular calcium propagation velocity at different times following MI.

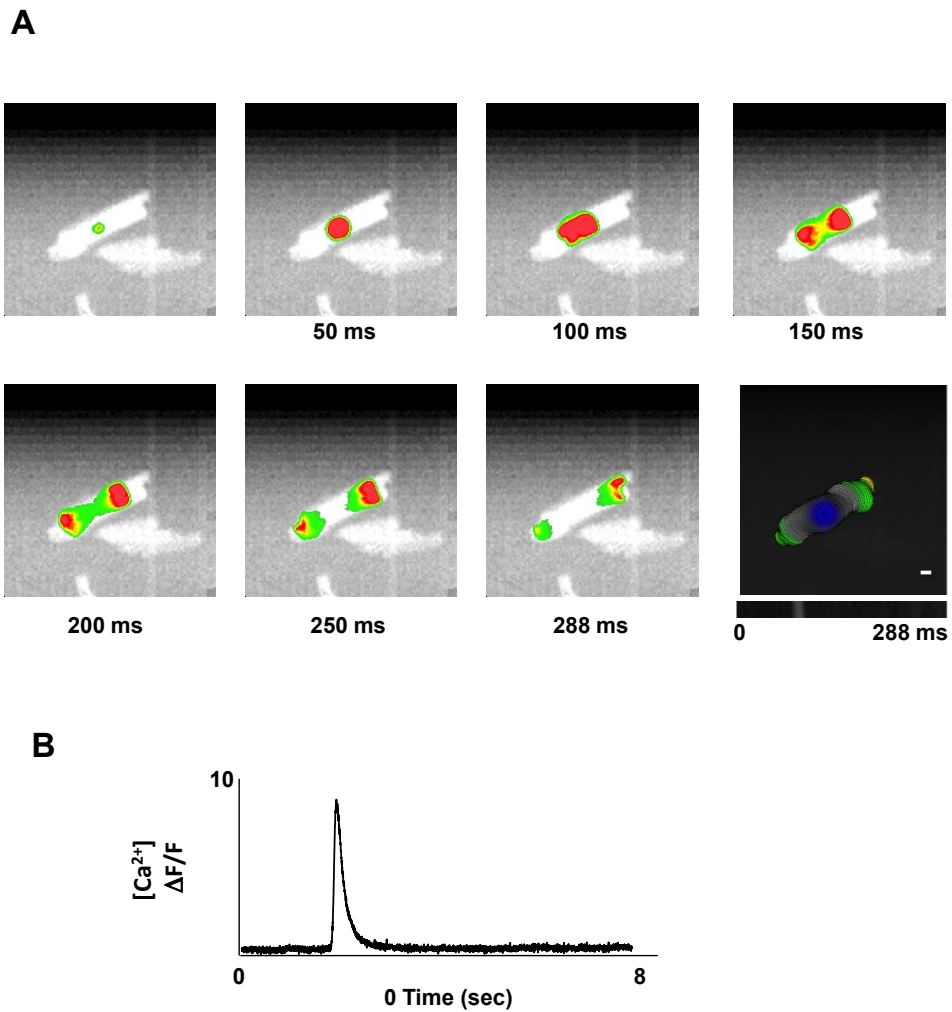


**Figure S2**

**Figure S2**, related to Figure 3

**Inhibition of mechanosensitive ion channels does not stop MiCa<sub>i</sub> initiation.** The cardiomyocytes were exposed to 30  $\mu\text{mol/L}$  gadolinium. **A.** Representative frames (time interval 50 ms) of MiCa<sub>i</sub> initiated at the pressure site (upper left) and propagated as ripple effect toward the cell edges; bottom right: isochronic color-coded map). **B.** MiCa<sub>i</sub> trace for the cardiomyocyte exposed to gadolinium shown in A. Scale bar 10  $\mu\text{m}$ , n=6.

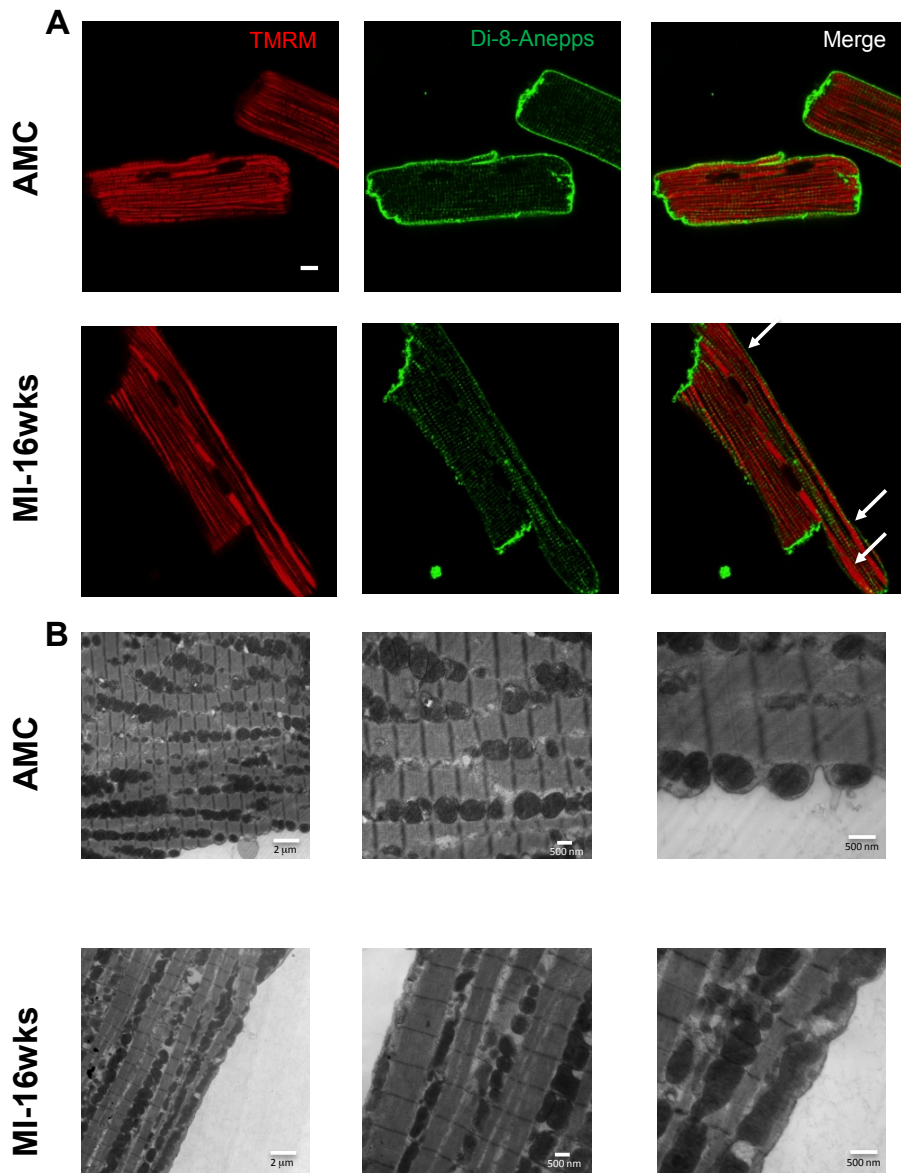


**Figure S3**

**Figure S3**, related to Figure 4

**Remodelling of mitochondria and T-tubule network following MI.** **A.** Mitochondria are stained with TMRM; T-tubules are stained with Di-8-ANEPPS in AMC myocytes (top row) and failing cells (bottom row). Bar= 10  $\mu$ m. Arrows indicate mitochondria enlargement and relocalization. **B.** Mitochondria organization displayed in TEM images for control cardiomyocytes (AMC, top) and failing cardiomyocytes (HF, bottom) showing mitochondrial enlargement at different magnification (from left to right 5000X, 10000X, 20000X).

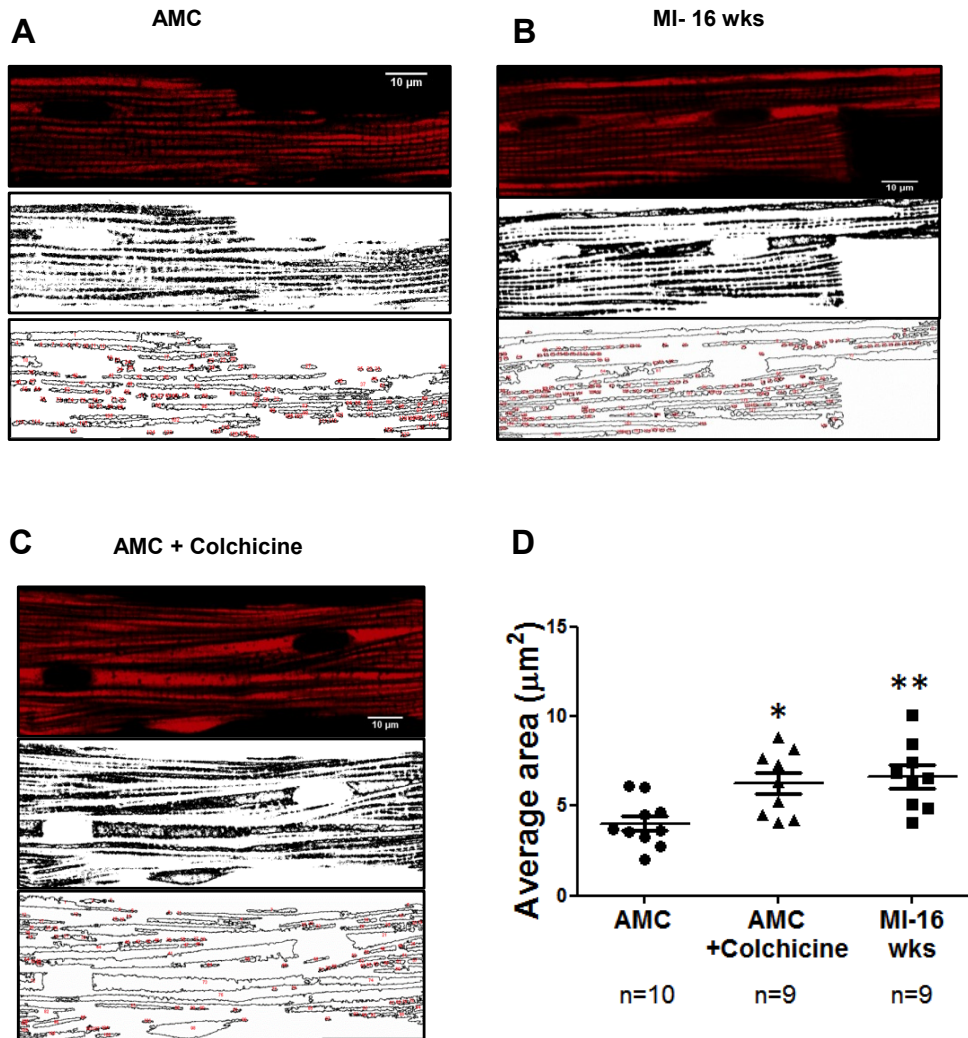


**Figure S4**

**Figure S4**, related to Figure 4

**Estimation of mitochondrial elongation.** **A.** Top: confocal image of a normal cardiomyocyte with mitochondria labeled (TMRM). Middle: the same image binarized. Bottom: regions of interest automatically selected for area calculations by a plug-in in ImageJ software. **B.** Same as A for a control cardiomyocyte exposed to colchicine. **C.** Same as A for a heart failure cardiomyocyte. **D.** Analysis of mitochondrial area in the three conditions: control, control+colchicine and heart failure.  $n > 9$ .  $P < 0.05$ .

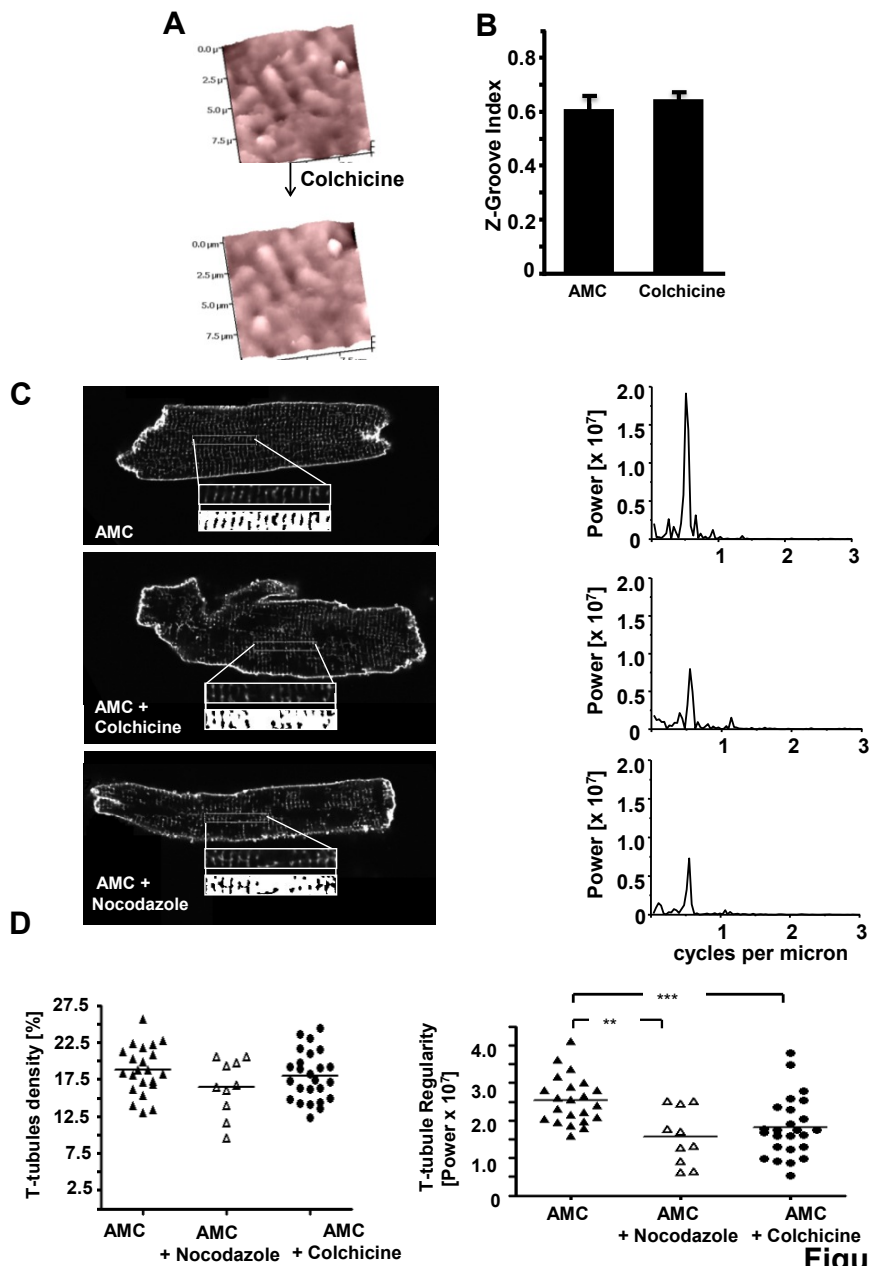


**Figure S5**

**Figure S5**, related to Figure 5

**Effect of Colchicine on T-tubules and Z-grooves** **A.** Topography of an AMC cardiomyocyte after treatment with colchicine (10  $\mu\text{mol/l}$ ). **B.** Z-groove index after colchicine treatment does not change; **C.** Left: T-tubule staining with Di-8-ANEPPS after colchicine or nocodazole treatment. Insets: binarised images of selected areas on which regularity calculations have been made; Right: Power of regularity of intensity peaks corresponding to the images on the left (fast Fourier Transform analysis); **D.** T-tubule density (left panel) and regularity (right panel) after colchicine or nocodazole treatment.

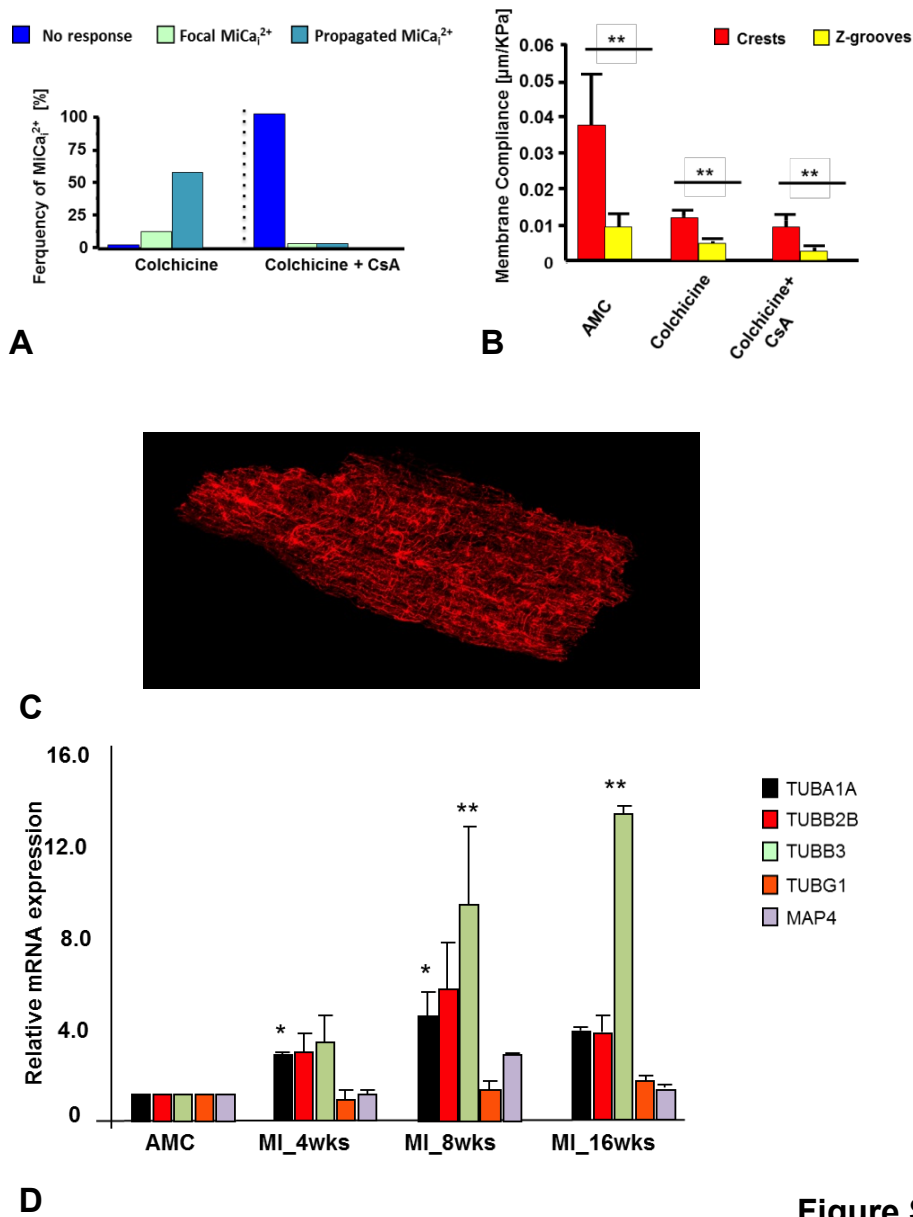


**Figure S6**

**Figure S6**, related to Figure 3 and 5

**Cyclosporine A abolishes  $MiCa_i$  after colchicine treatment but does not affect membrane compliance.** **A.** Occurrence of  $MiCa_i$  events in control cells subjected to colchicine and colchicine plus CsA. **B.** Membrane compliance of Z-grooves and crests in control cells, control cells subjected to colchicine and to colchicine plus CsA.

**Changes in tubulin expression in HF.** **C.** Representative image of a cardiomyocyte at 16 weeks post-MI stained for  $\beta$ -tubulin. Scale bar is 10  $\mu\text{m}$ . **D.** Relative mRNA expression for various microtubule proteins in: age matched control AMC, and different times following MI. (n=3 x technical triplicate normalized against Cyclophillin).

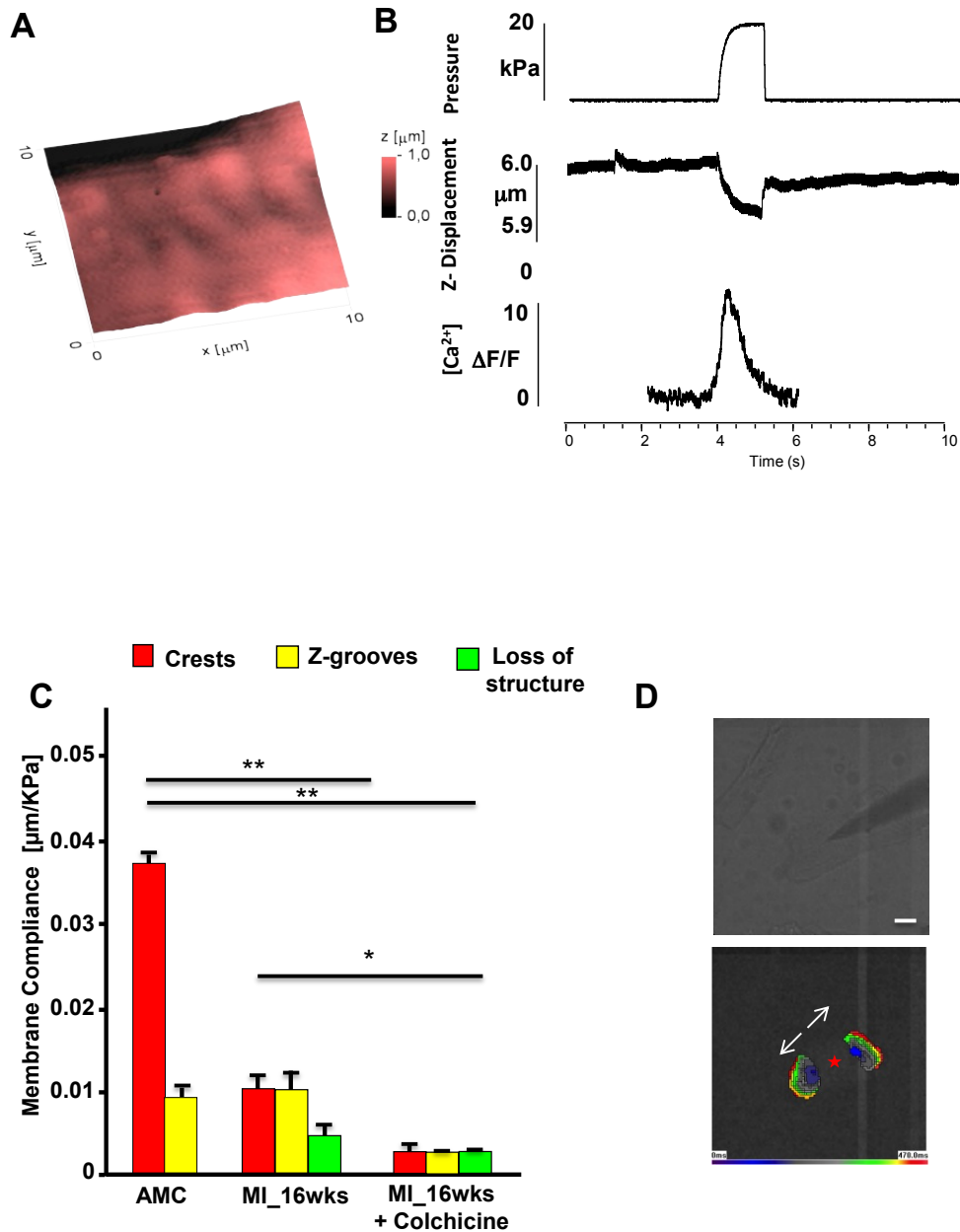


**Figure S7**

**Figure S7**, related to Figure 5

**Effect of microtubular network derangement in failing cardiomyocyte.** **A.** Representative SICM topographical image of a HF cell after colchicine treatment; **B.** Traces of mechanical application (top) membrane indentation (middle) and  $\text{MiCa}_i$  transient (bottom) in failing cardiomyocytes subjected to colchicine. **C.** Membrane compliance measurement in control cardiomyocytes (AMC), failing cardiomyocytes and failing cardiomyocytes subjected to colchicine. **D.** Top: nanopipette positioned on top of a cardiomyocyte for pressure application and (bottom) isochronic color-coded map of a subsequent  $\text{MiCa}_i$  event.



Weeks Post MI	n	HW (mg) / TL (mm) [mean (SEM) ]	n	LVEF (%)
Control	10	36.4 (2.07)	9	78.5 (3.21)
4	16	41.0 (1.10) *	5	53.5 (6.96)**
8	9	40.1 (1.43)	8	36.76 (5.90)***
16	16	46.5 (1.89) **	9	29.4 (2.02)***

**Table S1**

**Table S1**, related to Figure 2.

**Validation of the heart failure model by generating myocardial infarction with coronary artery occlusion.**

Heart weight/Tibia length ratio (HW/TL) and left ventricular ejection fraction (LVEF) in rats measured at 4, 8 and 16 weeks after coronary ligation. \*\* P<0.05 and \*\*\* P<0.01

<b>Rat Cell Type</b>	<b>MiCa<sub>i</sub></b>	<b>Surface structure</b>	<b>Membrane Compliance in Crest / Groove / Unstriated regions (μm/kPa)</b>	<b>Z-Groove Ratio, % change from AMC cells</b>
<b>AMC</b>	Focal at Z-Grooves	Regular	0.037 / 0.009 / -	100
<b>AMC + Colchicine</b>	Focal at Z-Grooves  Propagated at crests	Regular	0.01. / 0.005 / -	Unchanged
<b>AMC + Colchicine + CCCP</b>	None	Regular	0.014 / 0.006 / -	Unchanged
<b>MI-4 wks</b>	Focal at Z-Grooves;  Propagated with single initiation	Loss of some structures	0.009 / 0.006 / 0.003	-6.8
<b>MI-8 wks</b>	Propagated with triple initiation	Non-striated	0.008 / 0.015 / 0.010	-24.7
<b>MI-16 wks</b>	Propagated with triple initiation	Non-striated	0.010 / 0.010 / 0.013	-29.8
<b>MI-16 wks + Colchicine</b>	Propagated with triple initiation	Non-striated	0.003 / 0.002 / 0.003	-28.8
<b>MI-16 wks + Gd<sup>3+</sup></b>	Propagated with single initiation	Non-striated	0.015 / 0.010 / 0.011	-27.9
<b>MI-16 wks + CCCP</b>	none	Non-striated	0.008 / 0.006 / 0.001	-30.3

**Table S2, related to Figure 3. Summary of different conditions where we observed MiCa<sub>i</sub>**

## **Supplemental Movie Legend**

**Movie S1.** Pattern of  $MiCa_i$  propagation in MI\_16wks cardiomyocytes: single initiation

**Movie S2.** Pattern of  $MiCa_i$  propagation in MI\_16wks cardiomyocytes: multiple initiations.

**Movie S3.** Inhibition of mechanosensitive ion channels allows only single initiation of  $MiCa_i$ .

## **Supplemental Experimental Procedure**

### In-vivo cardiac function

Cardiac function was assessed via biometrics and echocardiography. Heart weight corrected to tibia length provided a measure of hypertrophy. Echocardiography was performed under general anaesthesia (2% isoflurane) immediately prior despatch to give a measure of in-vivo cardiac function. The imaging was performed in M-Mode in the parasternal long axis view (Table S1, Vevo 770 system). After 4, 8 or 16 weeks following coronary ligation, rats were despatched by cervical dislocation after brief exposure to 5% isoflurane until the righting reflex was lost. We perfused the left ventricle (LV) via the Langendorff perfusion apparatus<sup>1</sup>. Cardiomyocytes were enzymatically isolated from the LV.

### Topographical images

High-resolution cell membrane topography was achieved using high-resistance nanopipette (100M $\Omega$ ). Surface topographical images (10x10  $\mu$ m, 512x512 pixels) of the cardiomyocytes were acquired by the SICM at 25°C, pH=7.4. In order to avoid contraction and the same preparation was superfused with HBSS, pH=7.4 at 36 °C afterwards. After acquiring the topography image, the pipette was moved to a selected location on the cell surface 200 nm above a cell crest or groove by a controlled movement of the piezo drive.

### Transmission electron microscopy

Isolated cells were fixed in 2.5% glutaraldehyde in cacodylate buffer, cell pellets were embedded in 2% agarose and re-fixed in 2.5% glutaraldehyde, post-fixed in 1% osmium trioxide and embedded in Araldite following standard protocol. Ultra-thin sections were mounted on grids and stained for 7 minutes with 2% uranyl acetate in methanol, washed again in methanol, and stained for 5 minutes with 1% lead citrate in water and washed in water afterwards. The sections were observed with transmission electron microscope.

### Immunostaining

Adult cardiomyocytes were stained for  $\beta$ -tubulin (Monoclonal Anti- $\beta$ -Tubulin; t5201; Sigma-Aldrich; Alexa 546 anti-mouse immunoglobulin; Abcam) by a standard indirect immunofluorescence protocol. Cells on coverslips were fixed in 4% paraformaldehyde in PBS for 10 minutes, permeabilized in 1% triton X100 in PBS for 20 minutes; washed in PBS twice, incubated in blocking solution (5% BSA, 20% Newborn calf serum, 0.05% Tween 20 in PBS) for 30 minutes. They were then incubated with first antibody (diluted 1:100) in blocking solution overnight, washed in PBS twice, incubated with secondary antibody (diluted 1:100) in blocking solution for 30 minutes. They were subsequently mounted in Vectashield mounting medium (Vector Labs), sealed with nail varnish, and observed with confocal microscope (Zeiss LSM-780).

### **Supplemental reference.**

1. Sato M, O'Gara P, Harding SE, Fuller SJ. Enhancement of adenoviral gene transfer to adult rat cardiomyocytes in vivo by immobilization and ultrasound treatment of the heart. *Gene Ther.* 2005;12:936-941